ULTRASTRUCTURE OF PORE COMPLEXES OF ANNULATE LAMELLAE

GERD G. MAUL. From the Department of Pathology, Temple University School of Medicine, Philadelphia, Pennsylvania 19140

INTRODUCTION

Annulate lamellae (AL) have been described in various tissues of the animal kingdom (for review see reference 11). They consist of several paired double-membranes which are interrupted by regularly arranged pore complexes. The pore complexes appear structurally similar to nuclear pores (11, 13), and are described to be closed by a

diaphragm (2, 21) or to be patent (9, 10). At low magnification, electron-opaque, seemingly homogeneous material traverses the pores and extends a short distance into the cytoplasm, or connects adjacent pores (5, 6, 11). Recently (13) the pore complex of the nuclear envelope and AL were found to contain a matrix within which thin filaments and small granules were embedded which could aggregate in the center of the pore. The present report attempts to describe the pore complex of AL in melanoma cells in vitro, as the details differ significantly from those described by Kessel (13).

MATERIALS AND METHODS

Human melanoma cells in vitro were fixed in 3% glutaraldehyde in 0.1 M phosphate buffer (pH 7.4) at room temperature for 1 hr and postfixed in osmium tetroxide in the same buffer. Before rapid dehydration in a graded alcohol series, the cells were "prestained" in 0.5% uranyl acetate in water (8, 21). The cells were then flat-embedded (4) in Epon (15). Selected cells were sectioned on an LKB Ultrotome (LKB Instruments, Inc., Rockville, Md.), and the sections were stained with uranyl acetate and lead citrate (23). They were studied

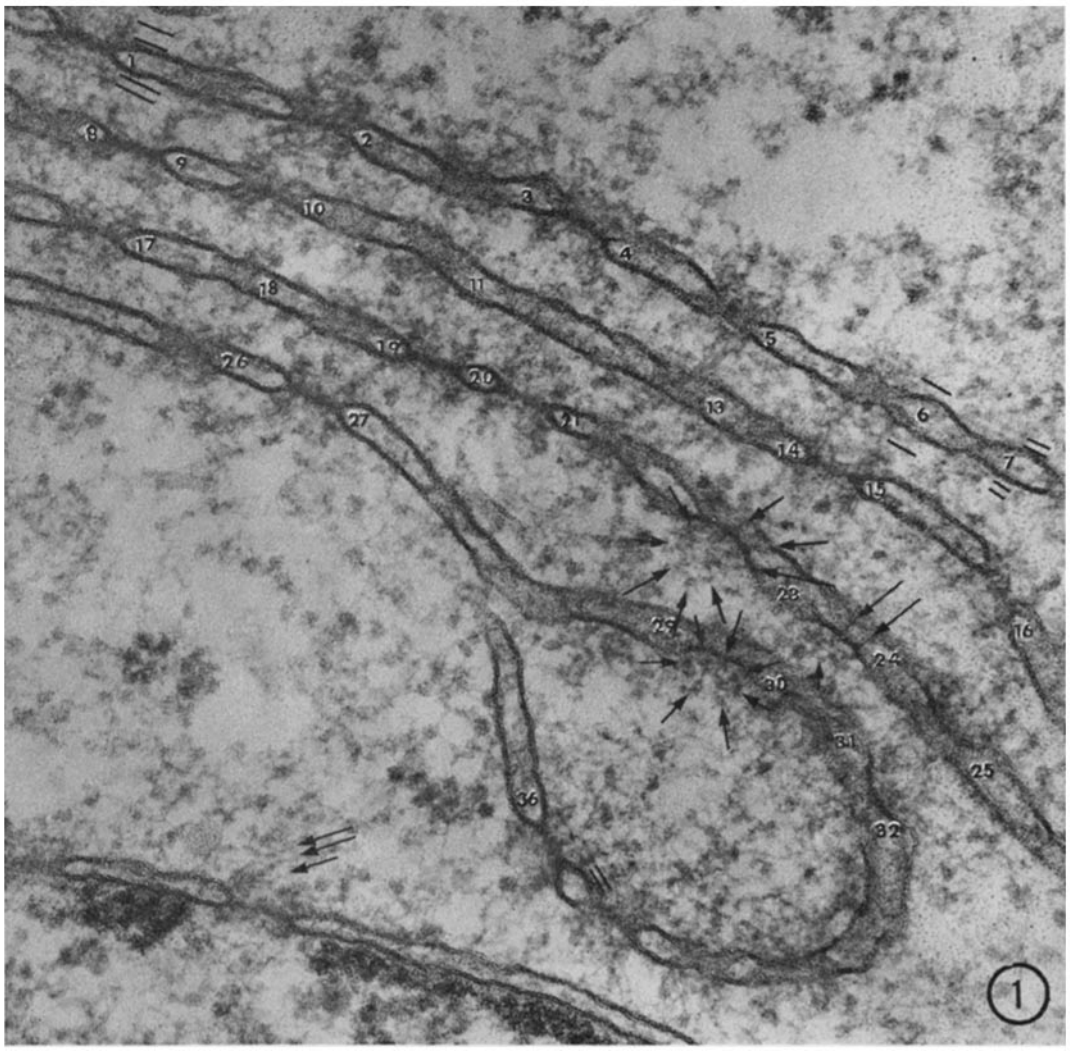

FIGURE 1 Micrograph of annulate lamellae showing pore complexes in cross-section and oblique section. Pores are numbered and their explanation is provided in the text. × 80,000.

with a Hitachi HU 11 C and a Siemens 101 electron microscope at 75 and 80 kv, respectively.

OBERVATIONS

Cross-sections of AL (Fig. 1) show pores in a variety of different angles, from nearly ideal cross-sections (pore 1) to near-tangential sections (pores 23, 24, 25, 29–32). Oblique sections are most helpful in determining the three-dimensional architecture of the pore complex, as they allow one to correlate structures seen in cross-sections and in face-on views of pores. Pores 1, 6, and 7 show two parallel lines "above and below" the pore (marked by black lines). The dark line closest to the pore is considered to be the projection of the rim of the pore (see also reference 3). Fibrous material traverses the pores and seems to be in continuity with fibers of other pores in registry (Fig. 1, between pores 6 and 15, and between pores 5 and 13). In nearly tangential pores (Fig. 1, pores 23, 30) it can be noted that the projection of these fibers suggests seven or eight single fibers (arrows). The pore rim (pore 24) shows two parallel lines suggestive of the corners of the angular pore outline (parallel arrows), and possibly of the superimposed traversing fibers. An oval-shaped ring is indicated by an arrow pointing up. The nuclear pore in the lower left corner shows three parallel fibers extending into the cytoplasm. They appear to be equivalent to the traversing fibers of AL pores.

The internal structure of the pore complex varies widely, as seen in face-on views. However, three types of arrangements or variations of them are most often found. They are depicted in Fig. 2 in the pore complexes 3, 5, and 6. Pore complex 3 shows a slightly acentrically located, somewhat angular ring with a diameter of approximately 250 A (long arrow pointing to its rim). This ring seems to be attached to the corners of the angular pore rim (short arrows). Pore complex 5 shows a ring structure closely apposed to the pore rim (short arrow). Four or five electron-opaque aggregates are localized in the center of the pore (dotted circle). Part of the ring structure closely apposed to the pore rim is also seen in pore complex 6, but the center is outlined by a central ring (approximately 100–125 A) which is surrounded by a structured matrix consisting in part of radiating fibers (upper right from the center of the pore complex). Pore complex 1 is only partly included in the section. A ring-like structure is seen acentrically (arrow).

FIGURE 2 Face-on views of the pore complex of AL. The central structures are seen in the center of pores 3, 5, and 6. The long arrow in pore complex 3 points to a fibrous ring approximately 250 A in diameter. The short arrows point to fibers which radiate from the inner fibrous ring to the pore rim. In pore complex 5 an arrow points to a ring structure closely apposed to the pore rim. Four or five electron-opaque aggregates are localized in the center of the pore (dotted circle). The arrow in pore complex 6 points to a center ring (approximately 100–125 A in diameter). × 222,000.

FIGURE 3 High magnification of a pore complex similar to pore 6 in Fig. 2. Arrows point to two ring-like fibers and to radiating fibers. × 300,000.

FIGURE 4 This pore complex corresponds to pore complex 3 in Fig. 2. It has an acentrically located ring-like fiber (arrow) which is attached to radiating fibers. × 125,000.

FIGURE 5 This pore complex corresponds to pore complex 5 in Fig. 2. Radiating fibers seem to connect to densities at the pore rim (projections of the traversing fibers). × 125,000.

FIGURE 6 Pore complex 1 shows part of a ring structure in the center (arrow). The pore rim (2) has an angular outline suggestive of octagonality. Pore complex 6 shows a seemingly more heavily stained halo around its membrane delimitation. × 158,000.

FIGURE 7 Projections of the traversing fibers are evident in the corners of the angular pores (arrows). × 158,000.

FIGURE 8 Selected pores were analyzed according to the method of Markham et al. (16). They showed strong enhancement of an octagonal symmetry and a very constant diameter. × 236,000.

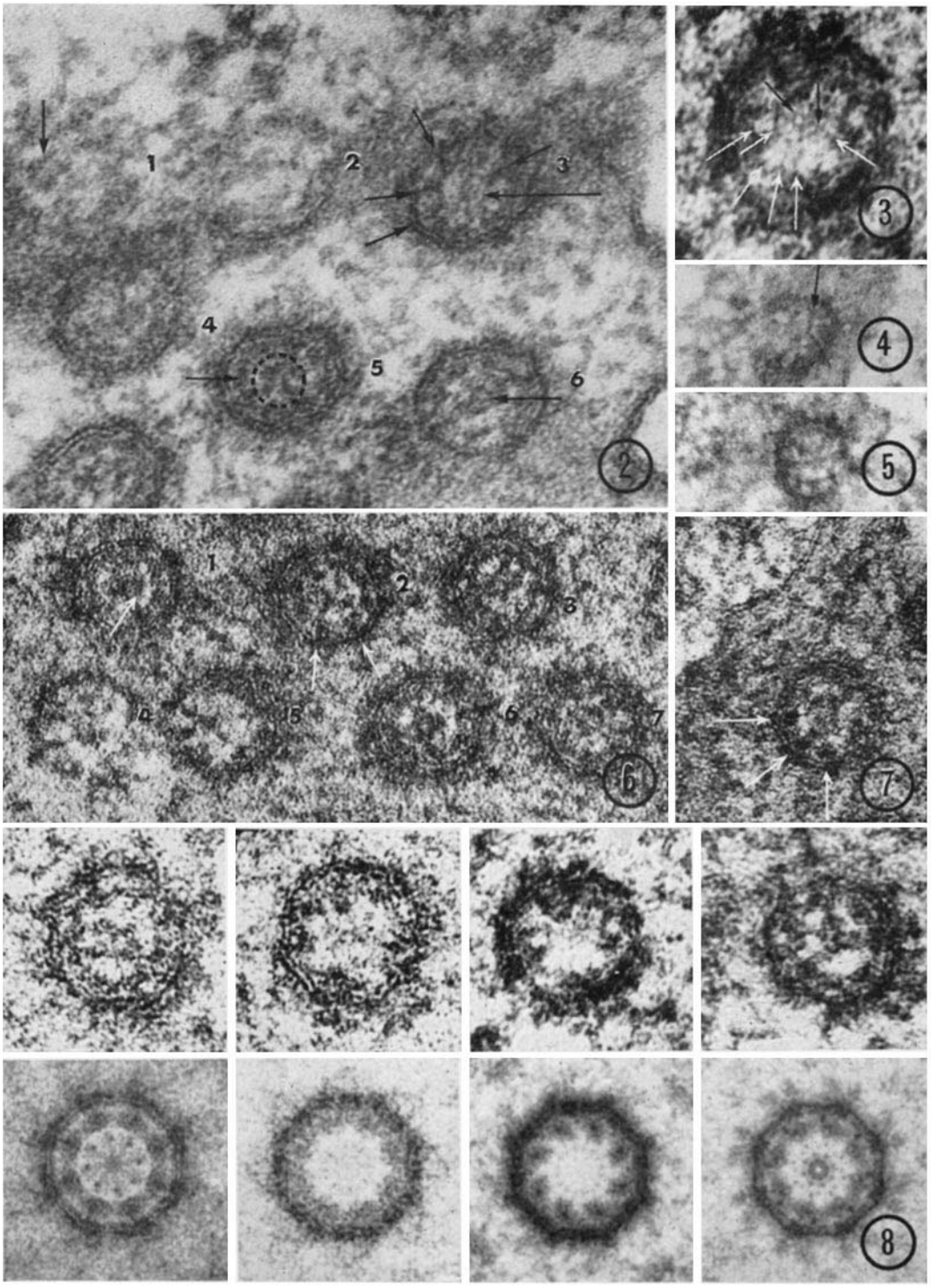

Pore complexes which appear patent at low magnifications seem to have very fine ring-like and radiating fibers and they resemble pore complex 6 in Fig. 2 (Fig. 3, black arrows point to ring-like fibers.). The center ring has a diameter of 40 A. An obliquely sectioned pore complex with a slightly acentrically located ring (approximately 250 A diameter) attached to radiating fibers is shown in Fig. 4. This pore complex corresponds to pore complex 3 in Fig. 2. The obliquely sectioned pore complex shown in Fig. 5 is similar to complex 5 (Fig. 2) and contains seven approximately equally spaced densities with radiating fibrous elements. The three densities at the lower part of the pore are connected by a fiber and appear to be a projection of the traversing fibers.

The pore complexes in Fig. 6 were found in a slightly overstained section, as is evident from their granular appearance. The pore complex seems to consist of randomly oriented fibers and granules similar to the ones described by Kessel (13). However, a ring-like structure is evident in pore complex 1. In pore complex 2 there are densities located in the lower part of the pore, and the pore appears octagonal. Pore complex 2 resembles pore complex 6, in that around the pore proper the membrane appears denser. This feature has been described previously (1, 7, 26, 27), but has been considered part of an "annulus", a feature which was not apparent in cross-sections in the material presented here. The pore complex in Fig. 7 demonstrates the electron-opaque structure in the corners of the angular pore (arrows), which is probably a projection of the traversing fibers seen in Fig. 1, pores 6, 15, and 16.

The angularity of the pore complexes in the AL is obvious and is suggestive of octagonality (see also references 7, 13, 18, 24, 28). This was tested by using the rotation printing method of Markham et al. (16). The printing stage was tilted to compensate for obliqueness of the pore in the section or for compression during sectioning. The short axis of the pore was increased to the length of the long axis. The results are shown in Fig. 8. There was strong enhancement of octagonal symmetry, and, of 20 pores rotated, 15 were octagonal. The rest were inconclusive partly because of failure to center the pore properly. A pore was considered properly centered when the three layers of the unit membrane could be seen in at least one of the prints of a series (i.e., n = 6, 7, 8, or 9). The pore diameter was remarkably equal in all rotated pores measured. The average of 15 pores was 790 A, measured from side to side after rotation printing. The distance between the opposite corners of the pores is 6.3% larger than the side-by-side distance. The diameter of the pore measured as a circle may therefore appear as much as 50 A larger.

DISCUSSION

Several investigations have been concerned with the ultrastructure of pore complexes of AL (12, 13, for review see reference 11). The structural similarities of pore complexes of AL and the nuclear envelope are striking, and no differences have been noted (13). Differences, however, should be expected because of the polarity of the nuclear pore complex caused by its relationship with chromatin.[1] The structure of the pore complex in the AL of human melanoma cells in vitro is very complex, and differs from the structure described for pore complexes in AL in oocytes of *Ophioderma panamensis* and *Orconectes virilis* (12), *Rana pipiens*, *Orconectes virilis*, and *Libellula pulchella* (13). In these oocytes the pores were described as containing annular material consisting of fibers and small granules which, it was proposed, aggregate into the central granule with the possible function of closing the pore to the passage of substances. This central granule was seen in less than 1% of the pore complexes of AL in human melanoma cells in vitro, and its position is the same as has been previously described (13). From analysis of the substructure of many pore complexes, it seems evident that there are not three types of pores, but that the three "types" described in Fig. 2 exhibit only the most strikingly organized substructures. A comparison with other pore complexes shows clearly that many intermediate stages exist. This may be due to functional differences or to different stages in a sequence of an as yet unknown function of the pore complex.

Common to most pores are the traversing fibers which may frequently be obscured by the position of the fiber relative to the electron beam. The traversing fibers of the nuclear pores in Fig. 1 would not appear as densities in a face-on view because they are bent. It cannot be resolved if the traversing fibers are attached to the pore rim. The number of subunits (8) in the pore complex was assumed to be the cause of its octagonality (25). Shrinkage around these subunits (which seem to be the equivalent of the traversing fibers), caused

[1] G. G. Maul and D. Branton. Manuscript in preparation.

by the dehydration process, however, would require a very rigid arrangement of the subunits or the traversing fibers. Replicas of freeze-cleaved preparations might solve the question of whether the dehydration process causes the octagonality of the pores. The position of a fibrous ring structure of 250 A diameter, off center, in an obliquely sectioned pore complex indicates that this structure is positioned "above" or "below" the pore proper. This ring structure was also found in the upper pore complex in Fig. 4, reference 13. Added evidence comes from the cross-sections of pore complexes showing two parallel lines above and below the pore complex. One of these may be due to the projection of a part of the pore rim (3), and the second to the projection of the ring. This fibrous ring structure is seemingly connected to the traversing fibers.

Ring structures approximately 40 A in diameter (Fig. 3) and 100–125 A in diameter were usually seen in the center of the pore, indicating their position at the level of the pore rim. They may be part of the "diaphragm" described previously for nuclear pores (2, 20, 22). The thick radiating fibers in the pore complex in Fig. 5 may correspond to the central densities in pore complex 5, Fig. 2. They may represent collapsed traversing fibers or intermediate stages in the ring formation or in the formation of the central granule. As it may be, they appear too frequently to be considered random precipitation products.

The ring structure closely apposed to the membrane of the pore can be seen in most pore complexes. However, it is less obvious in areas where the traversing fibers are well resolved. Therefore, it is assumed that part of the electron opacity of this ring is due to oblique traversing fibers. This is particularly evident in Fig. 6, pore complex 2, where the upper left of the pore shows this ring or annulus. At the lower right of the pore, the traversing fibers are resolved (arrows). This structural arrangement was first described as annulus and subannuli in isolated plant nuclei by Yoo and Bayley (29). However, they could not find "the extensions of the pores into the cytoplasm and nucleoplasm," which has been reported for nuclear pores (1). These extensions may well correspond to the traversing fibers as also reported by Chambers and Weiser (5, 6). The dense halo around the pore complex as is demonstrated in Fig. 6, pore complex 6, was attributed to the annulus in nuclear pores (7, 13), and to pore complexes of AL (12). This idea cannot be disproved, mainly because of the report of negatively stained detached annuli (7). However, an alternative explanation seems possible, if one assumes that the membrane appears denser as it becomes more and more parallel to the electron beam. Collapsed traversing fibers, though, may contribute to the annular appearance of the negatively stained preparations (7, 24, 28, 29).

The structural description does not allow any speculation about a possible function of the pore complex in AL (17). The observation of AL in basophilic bodies of the oocytes of *Libellula pulchella* (14), which presumably consist of RNA, and the digestion experiments performed on nuclear pore complexes with ribonuclease (20), suggest that part of the pore complex (central granule and annulus) consists of RNA.

This research was supported in part by grant CA-11654 from the National Institute of Health.

Received for publication 31 October 1969, and in revised form 4 March 1970.

REFERENCES

1. AFZELIUS, B. A. 1955. *Exp. Cell Res.* **8**:147.
2. BALINSKY, B. I., and R. J. DEVIS. 1963. *Acta Embryol. Morphol. Exp.* **6**:55.
3. BARNES, B. G., and J. M. DAVIS. 1959. *J. Ultrastruct. Res.* **3**:131.
4. BRINKLEY, B. R., T. MURPHY, and L. C. RICHARDSON. 1967. *J. Cell Biol.* **35**:279.
5. CHAMBERS, V. C., and R. S. WEISER. 1964a. *J. Cell Biol.* **21**:133.
6. CHAMBERS, V. C., and R. S. WEISER. 1964 *a. Cancer Res.* **24**:693.
7. GALL, J. G. 1967. *J. Cell Biol.* **32**:391.
8. KELLENBERGER, E., A. RYTER, and J. SECHAND. 1958. *J. Biophys. Biochem. Cytol.* **4**:671.
9. KESSEL, R. G. 1965. *J. Cell Biol.* **24**:471.
10. KESSEL, R. G. 1966. *Acta Embryol. Morphol. Exp.* **9**:1.
11. KESSEL, R. G. 1968. *J. Ultrastruct. Res. Suppl.* **10**:1.
12. KESSEL, R. G. 1968. *J. Cell Biol.* **36**:658.
13. KESSEL, R. G. 1969. *Z. Zellforsch. Mikrosk. Anat.* **94**:441.
14. KESSEL, R. G., and H. W. BEAMS. 1969. *J. Cell Biol.* **42**:185.
15. LUFT, J. H. 1961. *J. Biophys. Biochem. Cytol.* **9**:409.
16. MARKHAM, R., S. FREY, and G. J. HILL. 1963. *Virology.* **20**:88.
17. MAUL, G. G. 1970. *J. Ultrastruct. Res.* **30**:368.
18. MAUL, G. G. 1968. *J. Cell Biol.* **39**:88 *a.*
19. MENTRE, P. 1969. *J. Microsc.* **8**:51.

20. MERRIAM, R. W. 1959. *J. Biophys. Biochem. Cytol.* **5**:117.
21. PALADE, G. E., and R. R. BRUNS. 1968. *J. Cell Biol.* **37**:648.
22. REBHUN, L. I. 1961. *J. Ultrastruct. Res.* **5**:208.
23. REYNOLDS, E. S. 1963. *J. Cell Biol.* **17**:208.
24. SCHEER, U., and W. W. FRANKE. 1969. *J. Cell Biol.* **42**:519.
25. VIVIER, E. 1967. *J. Microsc.* **6**:371.
26. WATSON, M. 1955. *J. Biophys. Biochem. Cytol.* **1**:257.
27. WISCHNITZER, S. 1958. *J. Ultrastruct. Res.* **1**:201.
28. WUNDERLICH, F., and W. W. FRANKE. 1968. *J. Cell Biol.* **38**:458.
29. YOO, B. Y., and S. T. BAYLEY. 1967. *J. Ultrastruct. Res.* **18**:651.